Journal of Sustainable Civil Engineering and Technology
e-ISSN: 2948-4294 | Volume 5 Issue 1 (March 2026), 1-13
https://joscetech.uitm.edu.my
https://doi.org/10.24191/jscet.v5i1.JSCET_S_000036

Wide and Narrow-Spectrum Laser Ultrasonics for Fatigue Crack Detection Using Nonlinear Modulation Analysis

Nazirah Ab Wahab [1*] and Chindada Sony[2]

[1] Faculty of Civil Engineering, Universiti Teknologi MARA, 40450 Shah Alam, Selangor, Malaysia
[2]Institute of Thermomechanics of the CAS, v. v. i., Dolejškova 1402/5, 182 00 Praha 8, Czech Republic

[*]Corresponding author : nazirahwahab@uitm.edu.my

Received: 31 July 2025 / Accepted: 12 November 2025 / Published online: 31 March 2026

Abstract

Laser ultrasonic technique is widely applied in non-destructive evaluation (NDE) and structural health monitoring (SHM) for the broadband generation of ultrasonic waves. However, controlling the spectral content of the laser-generated waves can enhance the sensitivity of damage detection. In this study, a finite element model is developed to investigate how laser beam diameter influences ultrasonic wave generation. A small beam diameter is used to produce a wide-spectrum (WS) response, while a larger beam generates a narrow-spectrum (NS) response. The two independent ultrasonic responses are then combined to form a dual-laser excitation approach. When a structure contains fatigue damage, nonlinear ultrasonic modulation occurs between the WS and NS responses, leading to the generation of sidebands. A spectral energy-based index is employed to quantify these sidebands and identify fatigue-induced nonlinearity. The results confirm that the proposed dual-laser ultrasonics method improves sensitivity to fatigue cracks compared to conventional single laser excitation.

Keywords: Laser Ultrasonics, Nonlinear Ultrasonic Modulation, Finite Element Method, Fatigue Crack Detection, Structural Health Monitoring

1. Introduction

Irradiation of a specimen by a short laser pulse causes the surface to absorb the incident electromagnetic energy and undergo rapid localized heating. This heating increases the temperature gradient across the surface and the underlying material, prompting thermal expansion and the subsequent development of thermoelastic stresses. These stresses, acting as body forces, give rise to elastic (ultrasonic) waves that propagate outward into the specimen. The laser-induced ultrasonic generation technique has found wide application in non-destructive evaluation (NDE) and structural health monitoring (SHM), owing to its remote, non-contact operation and its ability to excite a wide range of frequencies (Scruby & Drain, 1990). Such capabilities are essential for examining components located in hazardous, confined, or otherwise inaccessible areas, as well as in high-throughput production environments where contact methods are impractical or would significantly obstruct the velocity of the inspection process (Yashiro, Takatsubo, Miyauchi, & Toyama, 2008) (Park, An, & Sohn, 2014) (Dixon, Burrows, Dutton, & Fan, 2010).

Evidence repeatedly illustrates the laser ultrasonic method's proficiency for identifying enfeeblement in both metallic and composite material systems, particularly when synergized with sophisticated signal-processing schemes, including frequency-wavenumber filtering and mode-dispersive isolation (Sohn, et al., 2011) (Ruzzene, 2007). Despite these successes, conventional linear ultrasonics remain limited when confronting nascent defects or submicroscopic flaws and could be insensitive to the early stage of fatigue crack development (Mezil, Chigarev, Tournat, & Gusev, 2016) (Liu, Sohn, & Park, Baseline-free damage visualization using noncontact laser nonlinear ultrasonics and state space geometrical changes, 2015). This limitation has prompted recent studies on nonlinear ultrasonic approaches, which exploit the crack-induced modulation generated by

alternating opening and closing of fatigue crack during wave propagation (Mezil, Chigarev, Tournat, & Gusev, 2016) (Liu, Sohn, & Park, Baseline-free damage visualization using noncontact laser nonlinear ultrasonics and state space geometrical changes, 2015) (Wagner, Mckie, Spicer, & Deaton Jr, 1990) (Baldwin, Berndt, & Ehrlich, 1999).

In nonlinear ultrasonic modulation, two distinct frequency inputs are combined to induce nonlinear interactions in a damaged structure. Traditionally, this is achieved by applying a low-frequency input and a high-frequency input simultaneously to a specimen containing fatigue damage, enabling the generation of sidebands and intermodulation components that serve as damage indicators. For instance, fatigue cracks in aluminum plates have been detected by applying a low-frequency input using a piezoelectric stack actuator in conjunction with a high-frequency input generated by a surface-mounted piezoelectric transducer (Liu, Jang, & Sohn, Fatigue crack detection using dual laser induced nonlinear ultrasonic modulation, 2018). Similarly, nonlinear modulation responses arising from fatigue cracks in aluminum alloys have been investigated using two obliquely incident shear transducers to generate low- and high-frequency ultrasonic waves under cyclic loading conditions (Liu, Jang, & Sohn, Fatigue crack detection using dual laser induced nonlinear ultrasonic modulation, 2018) (Liu & Sohn, Development of nonlinear spectral correlation between ultrasonic modulation components, 2017). Furthermore, this technique has been successfully employed in heterogeneous materials such as concrete, where an impact hammer has been used to introduce a low-frequency excitation while a piezoelectric transducer generates a high-frequency input, allowing the detection of microcracking and material deterioration (Liu, Sohn, Kundu, & Yang, 2014) (Huang, Krishnaswamy, & Achenbach, 1992) (Murray, Deaton Jr, & Wagner, 1996).

Recent advancements continue to strengthen the role of nonlinear ultrasonics and hybrid methods in fatigue crack detection and material evaluation. For example, the thermal modulation of nonlinear ultrasonic waves has been explored as a novel approach to enhance sensitivity in elastic media, offering improved non-destructive evaluation (NDE) capabilities (Zhu, Zeng, Malone, Tu, & Sun, 2025). Similarly, hybrid approaches that combine ultrasonic pulse velocity with nonlinear ultrasonic techniques have demonstrated promise in assessing concrete strength, thereby addressing limitations of conventional single-mode testing (Alnuaimi, Amjad, Alnuaimi, & Kundu, 2025). These recent contributions highlight the continuous relevance and expansion of laser-based nonlinear ultrasonics in structural health monitoring, underscoring the timeliness of the dual-laser approach investigated in this study.

Unlike prior nonlinear ultrasonic studies that depend on experimentally synchronized dual-frequency excitation and reference data from intact specimens, this study introduces a computationally efficient, baseline-free dual-laser finite element model that allows independent control of beam spectra (WS and NS). This distinction enables more precise assessment of fatigue-induced nonlinearities without the logistical constraints of conventional laboratory setups. While previous studies have successfully demonstrated nonlinear ultrasonic modulation for fatigue crack detection, these approaches generally rely on either synchronized low- and high-frequency sources or baseline reference measurements for comparison. Such requirements limit their practicality for in-situ monitoring, particularly in cases where reference data from an undamaged state is unavailable. In contrast, the present study advances the field by introducing a dual-laser finite element framework that generates wide-spectrum (WS) and narrow-spectrum (NS) responses independently and then combines them synthetically to emulate nonlinear modulation. This baseline-free approach improves detection sensitivity to fatigue-induced nonlinearities while eliminating experimental dependencies, thereby providing a more controlled and flexible platform for structural health monitoring.

Building on these advancements, the present study investigates the influence of laser beam diameter upon the efficacy of ultrasonic wave generation, simultaneously evaluating the beam's capacity for nonlinear modulation of the ultrasonic signal, with the ultimate objective of accurately locating and characterizing fatigue-induced microcracks. The analytical framework treats two laser geometries: a finite-radius, collimated beam designed for wide spectrum (WS) response, and a larger-radius beam for narrow-spectrum (NS) response. Instead of the simultaneous dual laser approach common in previous studies, this work iterates isolated finite-element

simulations of the WS and NS regimes. Subsequently, it combines the resulting wavefields, thereby recreating nonlinear modulation. This separation of wavefields eliminates the requirement for empirical baseline signals, enabling a rigorously controlled numerical investigation of fatigue-related nonlinear phenomena. The principal contributions of this research include: (1) a systematic study of how laser beam size affects ultrasonic wave propagation using finite element analysis; (2) the development of a method to combine WS and NS signals virtually, simulating dualbeam nonlinear interactions; and (3) the introduction of a spectral-energy approach to identify damage-related sidebands, enabling fatigue crack detection without the need for baseline reference data. The paper is organized as follows: Section 2 presents the finite element modeling of laser-induced ultrasonic generation and its validation against experimental data. Section 3 describes the nonlinear modulation framework for fatigue crack detection and the corresponding numerical results. Finally, Section 4 provides the conclusions and outlines directions for future research.

2. Research Method

2.1 Numerical Simulation of Laser Ultrasonic Wave Generation

Ultrasonic wave generation and subsequent wave propagation induced by a pulsed laser are examined numerically using the commercially available finite-element software, COMSOL Multiphysics. A two-dimensional axisymmetric formulation represents a semicircular aluminium plate of 75 mm radius and 3 mm thickness; a schematic of the geometry is provided in Figure 1. In the adopted coordinate system, the radial coordinate is denoted by r, and the coordinate associated with plate thickness is z. Material parameters incorporated into the computation are summarised in Table 1.

Pulsed laser excitation is simulated separately using two laser beam radii: 1 mm for wide spectrum (WS) excitation and 8 mm for narrow-spectrum (NS) excitation. In each case, the laser beam is directed at the centre of the plate ($r = 0$), with the ultrasonic sensor placed 50 mm away from the excitation point along the radial direction. The computation is segmented into two regions to represent the generation of heat-induced waves and their elastic propagation: the thermal wave domain, which addresses both thermal diffusion and mechanical displacement, and the ultrasonic wave domain, which focuses solely on mechanical displacements. The laser pulse is approximated as a Gaussian surface heat flux, imparting 10 mJ of energy in a 12 ns interval. The model assumes adiabatic boundary conditions at all external surfaces, maintaining thermal insulation to eliminate heat losses. The initial conditions are uniform, set at $T = 293.15$ K, with all mechanical displacements initialised to zero in both radial and axial directions. The initial condition of $T = 293.15$ K was chosen as it corresponds to standard laboratory room temperature, which is a common baseline in numerical modeling of laser-induced ultrasonics.

Journal of Sustainable Civil Engineering and Technology
e-ISSN: 2948-4294 | Volume 5 Issue 1 (March 2026), 1-13
https://joscetech.uitm.edu.my
https://doi.org/10.24191/jscet.v5i1.JSCET_S_000036

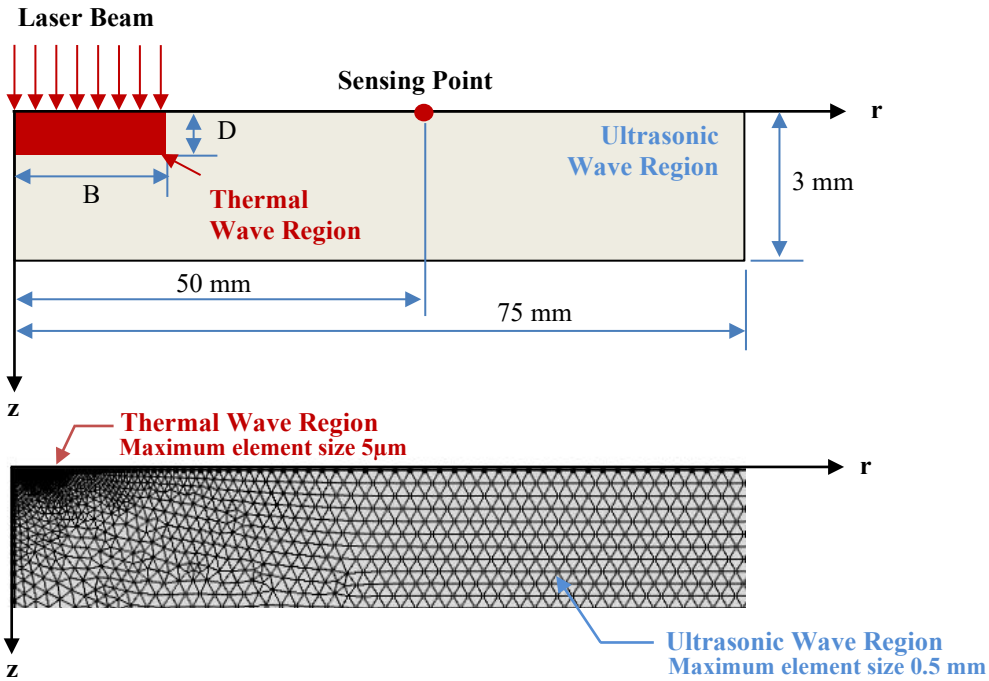

Figure 1. Schematic of the 2D axisymmetric model showing laser irradiation and FE mesh geometry.

Table 1. Properties of the aluminum used for numerical simulations.

Density ρ (kg/m^3)	Young's modulus E (GPa)	Poisson's ratio ν	Coefficient of thermal expansion α_t (K^{-1})	Thermal conductivity K (W/(m·K))	Heat capacity at constant pressure C_p (J/(kg·K))	Reflection coefficient R_C
2700	68.9	0.33	2.34×10^{-5}	170	900	0.95

Note: Material properties were adapted from standard values reported in (Liu, Nazirah, & Sohn, Numerical simulation of damage detection using laser-generated ultrasound, 2016) as no new material characterization was performed in this study.

The modeling strategy adopts a two-domain approach to capture thermal diffusion and elastic wave propagation accurately. The first domain, a narrow band around the laser focal spot, accounts for the interplay between evolving thermal fields and mechanical stress. The second domain, which extends outward into the free volume, treats the wave propagation as uncoupled elastodynamic motion. In the thermal wave domain, each computational node variable comprises one thermal and two mechanical degrees of freedom, while in the ultrasonic wave region, mechanical displacement alone is solved. A multi-scale mesh refinement policy is adopted to balance computational tractability and discretization fidelity. Triangular finite elements are employed throughout, with a localized body of finer mesh placed near the laser focus to resolve both the elevated thermal gradients and the attendant short-period elastic oscillations. The characteristic dimensions of the coarser and finer elements are calibrated to the relevant characteristic wavelengths, fixed at approximately 2 μm for thermal conduction and 0.1 mm for the ultrasonic regime, ensuring the numerical representation remains within the fidelity bounds of wave scattering and dispersion phenomena.

As illustrated in Figure 1, the thermal wave region in the finite element is represented by a radial width B and depth D. The area under consideration is quantitatively described through the thermal diffusion length, symbolized as μ_t. This length scale characterizes the spatial extent over which the magnitude of the thermal flux diminishes to roughly 37% of its initial amplitude at a specified instant t. The diffusion length is calculated based on thermal diffusivity κ, which is defined as the ratio of thermal conductivity K to the product of material density ρ and specific heat at constant pressure C_p (i.e. $\kappa = K/\rho C_p$).

Considering a laser beam radius of 1 mm and a pulse duration of 12 ns, the temporal analysis is timed to align with the point when the surface temperature recedes to less than 1% of the maximum attained during laser irradiation, occurring near 10 μs after the pulse. With a thermal diffusion length, μ_t, of 53 μm, the thermal wave volume exhibits a depth, D, of roughly 110 μm and extends radially to about 1110 μm. This investigation addresses how beam diameter influences the spectral content of ultrasonic waves generated via laser excitation. Numerical simulations are performed for both the weakly and the strongly dispersive regimes. The 1 mm configuration induces a tightly confined volumetric heating, leading to intricate waveforms encompassing a broad frequency spectrum. Conversely, the 8 mm wave beam displays progressively more sinusoidal shapes, dominated by lower frequency oscillations.

2.2 Validation of laser ultrasonic generation

A circular aluminum plate specimen with the same geometric dimension as the previous experimental testing conducted by (Liu, Nazirah, & Sohn, Numerical simulation of damage detection using laser-generated ultrasound, 2016) is constructed in finite element (FE) simulation. In this study, the velocity waveforms produced by the FE model for laser beam radius of 1mm and 8mm were compared against the published results from previous research. Validation is carried out in both the time and frequency domains, assessing consistency in overall spectral distributions, and the characteristics of frequency peaks. Velocity responses from the finite-element simulation are acquired at 50 mm from the excitation source and normalized. A Fast Fourier Transform is then employed to map the signals to the frequency domain, allowing direct spectral correspondence with the frequency results published by (Liu, Nazirah, & Sohn, Numerical simulation of damage detection using laser-generated ultrasound, 2016). This procedure calibrates the computational model, confirming that the computed waveforms and spectral content match observed experimental behavior. Following this validation, the model is applied to explore nonlinear ultrasonic modulation, thereby advancing the analysis of fatigue crack detection.

2.3 Nonlinear Ultrasonic Modulation for Fatigue Crack Detection

This study devised a numerical workflow to assess fatigue crack detection by nonlinear ultrasonic modulation, incorporating distinct finite element models for wide spectrum (WS) and narrow spectrum (NS) laser excitations. The WS component deployed a 1 mm beam waist, while the NS configuration employed an 8 mm beam. Each simulation operated within a common 2D axisymmetric finite element framework: the excitation was directed to a central point on the plate, and a designated sensing location was positioned 50 mm away from the beam focus. The velocity fields for the two beam geometries were calculated and output as data sets. They were then imported into MATLAB, where they were combined to formulate a synthetic signal exhibiting nonlinear modulation behavior.

Nonlinear modulation was defined via time-domain multiplication of the wide spectrum (WS) and narrow spectrum (NS) components. This approach mimics the collisional interplay of two laser beams traversing a medium harboring thermally induced nonlinearities, thus permitting the exploration of modulation signatures, sideband emission, and spectral widening, absent the logistical burden of synchronized twin laser sources. The output field was subsequently analyzed in the frequency domain, employing the Fast Fourier Transform (FFT) to derive a spectral representation. Close inspection of the spectral output revealed extraneous frequency bands flanking the WS carrier, interpreted as corroborative signatures of damage-linked nonlinear coupling. For a quantitative metric of the modulation manifestation, the Nonlinear Index (NLI) was formulated as:

$$NLI = \frac{\sum A(f)}{A(f_c)} \quad \text{(Equation 1)}$$

where $A(f)$ represents the spectral magnitude at frequency f, $A(f_c)$ is the spectral magnitude at the carrier frequency, and the numerator corresponds to the cumulative spectral energy within the upper and lower sidebands surrounding f_c. This index provides a direct measure of damage-induced nonlinear modulation, with higher NLI values indicating a stronger nonlinear response and, consequently, a higher likelihood of fatigue crack presence. The nonlinear index (NLI) is a ratio of spectral energies and therefore dimensionless and follows previous works on nonlinear modulation spectroscopy (Liu & Sohn, Development of nonlinear spectral correlation between ultrasonic modulation components, 2017).

Based on this dualbeam ultrasonic approach, fatigue crack detection is performed in the following steps and as shown in Figure 2; Step 1: Independent finite element analyses are carried out for wide spectrum (WS) and narrow spectrum (NS) excitations. The frequency spectra of the WS and NS responses are obtained, with the WS spectrum serving as the broadband reference and the NS spectrum used to define its lower-frequency content. Step 2: The WS and NS responses are combined to construct a modulation response. This synthetic signal emulates the nonlinear interaction between the two excitations that would occur in the presence of a fatigue crack. Step 3: The Fourier spectrum of the modulated response is computed. Nonlinear features, such as sidebands adjacent to the carrier frequency, are identified as indicators of damage-related modulation. Step 4: A nonlinear index (NLI) is calculated from the spectral energy in the sideband regions relative to the carrier frequency. An increase in NLI signifies the presence of crack-induced nonlinearities. This procedure, based entirely on simulated ultrasonic data, removes the need for baseline reference measurements, providing a robust and practical framework for fatigue crack detection.

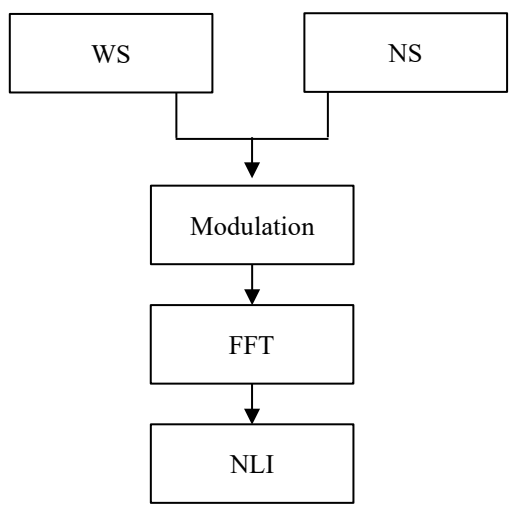

Figure 2. Schematic flow of the dual-laser nonlinear modulation process used in this study.

3. Results and Discussion

3.1 Validation of Finite Element Model

The developed finite element model was validated by comparing it with previously published experimental data on laser-induced ultrasound in aluminum plates. The original investigation employed a pulsed 1 mm beam

radius laser to generate waves and recorded out-of-plane velocities with a laser Doppler vibrometer (LDV). The resultant frequency spectra were then employed to characterize the thermoelastic response. Figure 3 shows contrasted frequency spectra from the experimental study and the present numerical model. The experimental data (on the left) reveal a broadband spectrum featuring pronounced peaks around 1 MHz, consistent with the simultaneous excitation of multiple guided wave modes. Such a spectral distribution emerges from the laser energy's highly localized and impulsive deposition, which is known to impart a wide range of frequency components into thin plates. The finite element results (right panel) replicate the experimental spectrum's qualitative shape and the strongest peaks within the observed bandwidth, thus confirming the model's capacity to capture essential excitation physics.

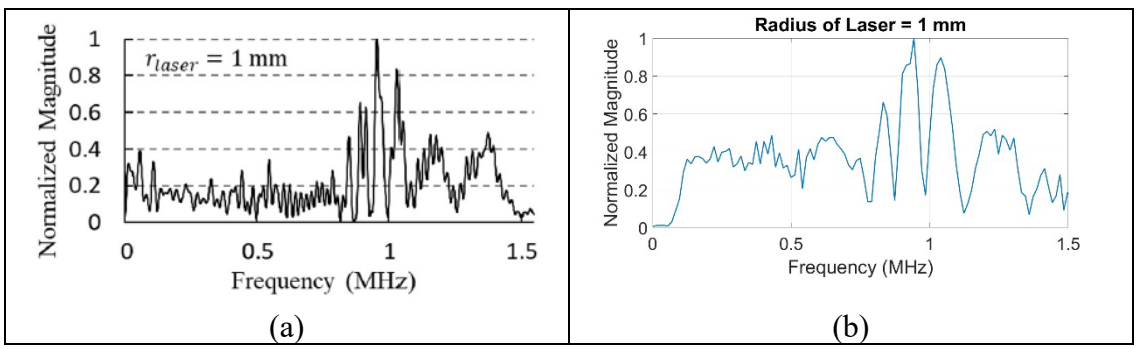

Figure 3. Comparison of normalized frequency spectra of out-of-plane velocity signals generated by a 1 mm laser beam radius: (a) experimental reference data adapted from (Liu, Nazirah, & Sohn, Numerical simulation of damage detection using laser-generated ultrasound, 2016); (b) finite element simulation result from this study.

By contrast, the finite element model (right) replicates the broadband spectral behaviour with outstanding fidelity, exhibiting principal frequency peaks centred around 100 kHz. Upon normalising the frequency axis to megahertz for direct juxtaposition, the FEM output shows qualitative correspondence with the experimental spectrum. Both datasets display analogous peak spacings, normalised intensities trending toward unity, and a harmonic-rich continuum spanning 0.05 to 0.2 MHz. The coexistence of well-defined spectral peaks and broadband emission corroborates that the simulation reproduces the fundamental physics of laser-induced ultrasonic wave transmission within the aluminium plate. Discrepancies in minor peak magnitudes and spectral smoothness are primarily attributed to the exclusion of experimental noise, surface waviness, and heterogeneities in the FEM formulation. Additionally, the experimental setup incorporates reflections from the boundaries and the limited response of the detection sensors, which are overlooked in the idealized computational model.

The consistent alignment in spectral shape, leading frequency components, and normalized amplitude variations demonstrates that the finite element model accurately captures the physical mechanisms governing laser-induced ultrasonic wave generation. As the model validated, it provides a robust platform for expanded parametric investigations, including the influence of laser beam diameter, complexities of wave interactions, and the sensitivity of fatigue crack detection across differing structural environments.

3.2 Effect of Laser Beam Size on Ultrasonic Frequency Response

The impact of laser beam diameter on the temporal and spectral properties of the resulting ultrasonic waves was assessed through finite element modeling, comparing beam radii of 1 mm and 8 mm. The time-domain velocity signals and their associated frequency distributions for each beam diameter are illustrated in Figure 4. The waveform corresponding to the 1 mm beam, labeled wide spectrum (WS) excitation and displayed in the uppermost plots, reveals a rapid, oscillatory velocity profile with a pronounced initial peak followed by clusters

of higher-frequency packets. Such a temporal signature signals the simultaneous excitation of multiple elastic wave modes resulting from the localized and rapid thermal expansion. The corresponding frequency spectrum extends from approximately 50 to 200 kHz, exhibiting distinct maxima near 100 kHz and a pronounced second-harmonic content. The extensive spectral content correlates with the steep thermal gradients produced by the narrow beam, which preferentially correspond to symmetric and antisymmetric Lamb wave propagation.

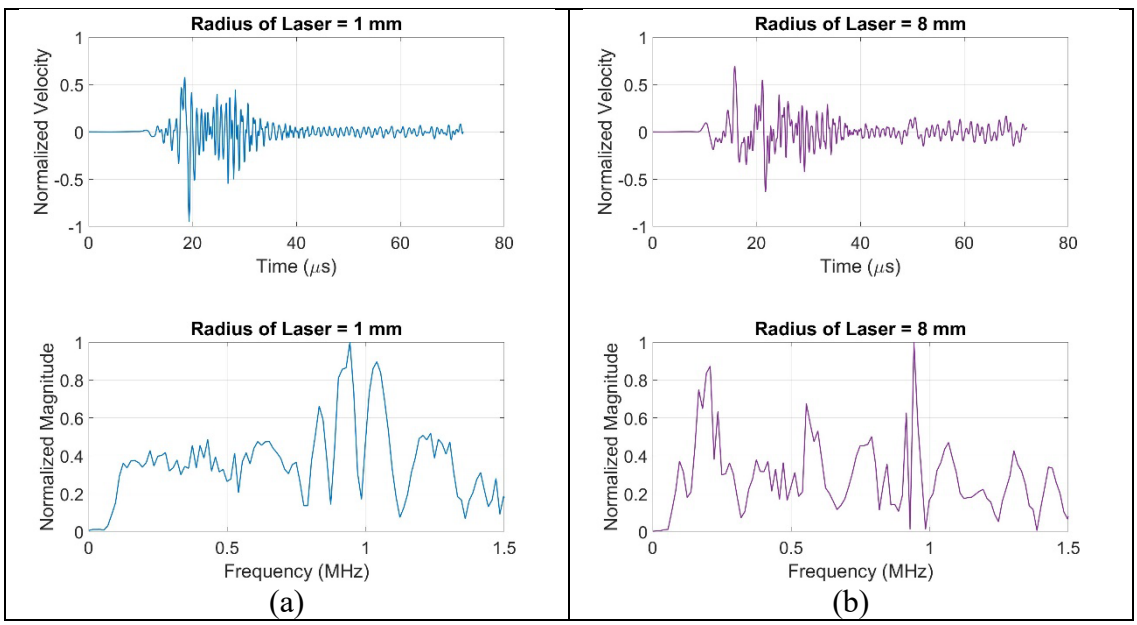

Figure 4. (a) Velocity response and FFT for WS excitation (1 mm radius); (b) Velocity response and FFT for NS excitation (8 mm radius).

In contrast, the lower section of Figure 3 shows the data recorded with an 8 mm beam radius, aligned with the narrow spectrum excitation. The time-domain signal is smoother, exhibiting diminished high-frequency amplitudes relative to the 1 mm setup. The milder spatial heating and more uniform thermal deposition from the wider beam diminish sharp thermal gradients, suppressing rapid transients and promoting lower-frequency modes. The corresponding frequency spectrum verifies this behaviour, presenting a principal peak at approximately 90–100 kHz and a markedly restricted bandwidth. The minimal presence of high-frequency content indicates weaker harmonic generation and a more confined spatial distribution of spectral energy. In Figure 4a, the velocity magnitude for the 8 mm radius laser is less concentrated between 1 and 2 MHz compared to the 1 mm case because the larger beam produces more uniform heating, which suppresses sharp thermal gradients. This results in weaker excitation of higher-frequency Lamb wave modes, hence lower intensity in this frequency band.

Furthermore, in Figure 4b, the FFT of the 8 mm radius beam shows a distinct first peak around 0.2 MHz, whereas no comparable peak occurs for the 1 mm beam. This can be explained by the wider thermal diffusion zone of the 8 mm laser, which preferentially excites lower-frequency fundamental modes, while the 1 mm beam couples more strongly into higher-frequency broadband modes.

The experimental outcomes demonstrate that the optical beam diameter significantly influences the frequency characteristics of the induced ultrasonic waves. A diminished beam radius produces a broader excitation spectrum, revealing subtle, damage-linked phenomena that might otherwise elude detection. In contrast, an increased beam radius confines the energy to discrete, selectively excited vibrational modes. The resulting beam-radius-dependent tuning of the spectral content thereby underpins the dualbeam nonlinear modulation strategy introduced herein.

3.3 Nonlinear Modulation Analysis for Fatigue Crack Detection

The data illustrated in Figure 5 provides the fast fourier transform spectra corresponding to the amplitude-modulated signals acquired under dual laser excitation in the 1 mm × 8 mm geometry. When the specimen remains intact, the spectrum reveals a dominant carrier frequency accompanied by a faint scattering of sidebands. It reflects a predominantly linear elastic behavior and the absence of considerable nonlinear phenomena. The spectrum obtained from the specimen in a damaged state shows expanded frequency clusters surrounding the central carrier, a behavior associated with nonlinear contact-acoustic phenomena resulting from micro-crack formation. Generating these peripheral frequency clusters constitutes a compelling signature of the progressively accumulating fatigue damage.

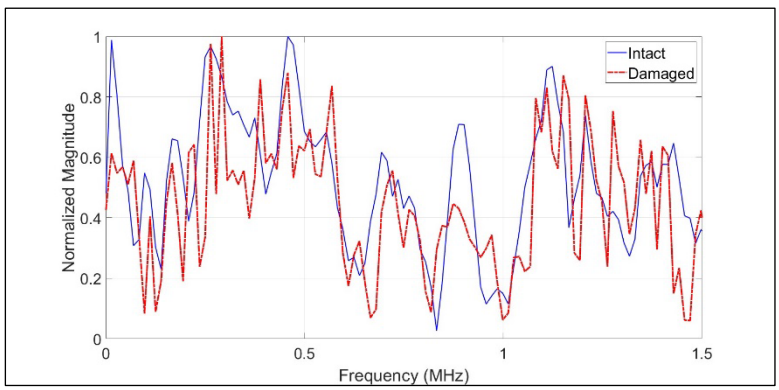

Figure 5. FFT spectra of the modulated signal (1 mm × 8 mm) for intact and damaged conditions.

Figure 6 presents a comparative analysis of the FFT spectra obtained from the independent excitations, specifically, the 1 mm wide spectrum beam and the 8 mm narrow spectrum beam, together with the resultant modulated signal. he WS excitation displays a broadband response with multiple frequency peaks, while the NS excitation exhibits a more concentrated, low-frequency spectrum. The modulated response, however, reveals a considerably enlarged frequency span and introduces additional features that the constituent excitations do not exhibit. This observation attests to frequency mixing and energy redistribution effects. The implementation of the dualbeam excitation protocol is thus shown to effectively isolate and enhance nonlinear interactions that are symptomatic of incipient fatigue damage. These interactions would remain undetected under a singular-beam approach.

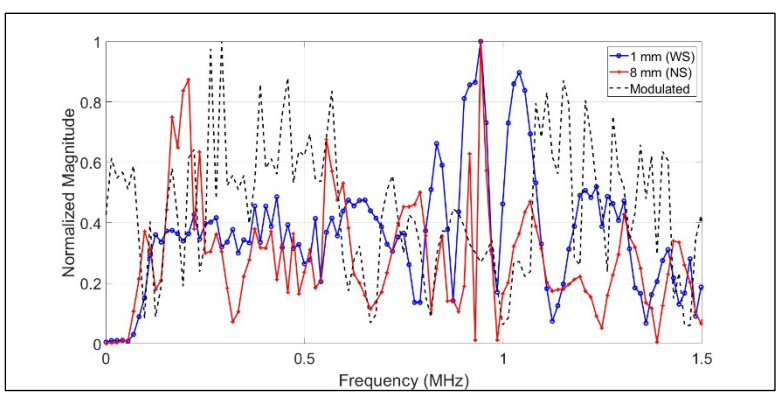

Figure 6. Comparison of FFT spectra for individual excitations (1 mm wide spectrum and 8 mm narrow spectrum) and the modulated signal (1 mm × 8 mm).

Quantitative assessment of the spectral modifications was accomplished by calculating the Nonlinear Index (NLI), presented in Figure 7. The NLI measured under the damaged scenario (99.15) markedly exceeds the figure recorded for the intact state (61.81), confirming the proposed modulation-based strategy's capacity to detect crack-induced nonlinearities. The magnitude of this disparity corroborates the validity of the duallaser modulation strategy for discriminating between intact and compromised structures, eliminating the requirement for reference measurements derived from the undamaged configuration. The nonlinear index (NLI) is a ratio of spectral energies and therefore dimensionless.

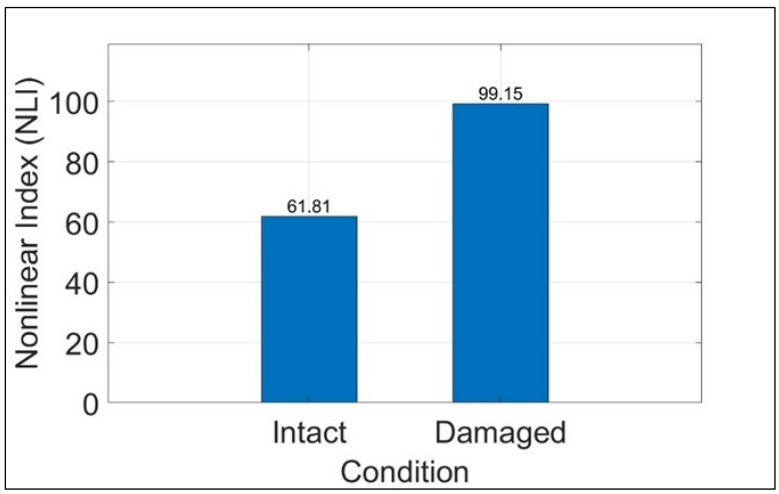

Figure 7. Nonlinear Index (NLI) comparison between intact and damaged conditions.

The NLI values provide a clear distinction between intact and damaged specimens. The intact condition exhibits an NLI of 61.81, corresponding to predominantly linear elastic wave propagation with minimal nonlinear coupling. In contrast, the damaged specimen records a substantially higher NLI of 99.15, reflecting enhanced nonlinear sideband generation due to crack opening and closure during wave interaction. The increment of 60 % in NLI represents a significant rise in nonlinear interaction strength, confirming the method's sensitivity to early fatigue-damage initiation.

Comparative evaluation with published benchmarks indicates that an NLI increment exceeding 30–40 % typically marks the onset of fatigue-induced micro-cracking (Zaitsev, Matveev, & Matveyev, 2009) (Liu & Sohn, Development of nonlinear spectral correlation between ultrasonic modulation components, 2017). The increment of 60% observed here therefore demonstrates high detection sensitivity, suggesting that the dual-laser modulation technique can identify crack initiation before macroscopic failure develops. It should be emphasized that NLI is not a normalized percentage but an absolute, dimensionless index; hence, the values for intact and damaged states do not sum to 100 but represent independent measures of nonlinear interaction strength.

From a structural-health-monitoring (SHM) perspective, the high contrast between the two NLI values establishes a quantitative detection threshold for practical field implementation. Even when conventional linear ultrasonic spectra show limited changes, the amplified NLI response provides a reliable indicator of micro-damage accumulation. Consequently, the dual-laser nonlinear modulation approach offers both theoretical insight into nonlinear wave interactions and a practical, baseline-free metric for early fatigue-crack detection in metallic components.

4. Conclusion

This study applied a finite element simulation platform to quantify how variations in laser beam diameter affect

ultrasonic wave generation and to demonstrate the method's sensitivity to fatigue crack detection via nonlinear modulation analysis. Specifically, the analysis compared wide-spectrum (WS) and narrow-spectrum (NS) emissions derived from 1 mm and 8 mm beam diameters. Results showed that beam radius significantly influences the spectral characteristics of laser-generated ultrasonic waves. The narrower 1 mm beam produced a high-frequency broadband response spanning 0.05–0.2 MHz, while the wider 8 mm beam generated a smoother, low-frequency spectrum centered near 0.1 MHz. The corresponding normalized velocity amplitude reached approximately 1.0, confirming the accuracy of the thermal–elastic coupling in the simulation.

A novel dual-laser nonlinear modulation strategy was developed through the numerical superposition of WS and NS signals. The computed nonlinear index (NLI) provided clear discrimination between intact and damaged conditions: the intact specimen exhibited an NLI of 61.81, while the damaged specimen reached 99.15 where an increment is nearly 60%. This significant rise in nonlinear interaction confirms the sensitivity of the dual-laser approach in identifying early-stage fatigue damage. The findings therefore demonstrate that the proposed framework can detect micro-crack development without requiring baseline reference measurements.

Beyond summarizing results, these findings also highlight the theoretical advancement of using beam-diameter-dependent laser excitation to control spectral content, offering a deeper understanding of how nonlinear modulation arises from local damage zones. However, the present work is limited to numerical simulations and does not include experimental validation. Physical testing under controlled laboratory conditions is essential to verify the model's predictive capability, particularly for real materials with surface roughness, thermal losses, or boundary reflections not fully captured in simulation.

Future work will focus on integrating the dual-laser nonlinear modulation concept into practical Structural Health Monitoring (SHM) systems. This includes developing an experimental dual-laser setup, optimizing excitation parameters for in-field applications, and exploring data-driven or AI-assisted methods to automatically identify significant NLI variations. Such efforts will enable this baseline-free approach to evolve from a simulation framework into a deployable nondestructive evaluation (NDE) technique suitable for fatigue monitoring in aerospace, transportation, and civil infrastructure systems.

Acknowledgments

The authors extend their gratitude to the Universiti Teknologi MARA for providing support through the Geran Penyelidikan MyRA 600-RMC/GPMLPHD 5/3 (009/2023).

Declaration of Conflicting Interests

All authors declare that they have no conflicts of interest.

Author Contributions

Conceptualisation, Nazirah Ab Wahab; Methodology, Nazirah Ab Wahab; Finite Element Simulation, Nazirah Ab Wahab; Validation and Analysis, Nazirah Ab Wahab and Sony Chindada; Writing – Original Draft Preparation and Review, Nazirah Ab Wahab and Sony Chindada. All authors have reviewed and approved the final version of the manuscript for publication.

Declaration of Generative AI in the Writing Process

During the preparation of this manuscript, the authors used generative artificial intelligence tools solely for language editing and grammar refinement. All intellectual content, analysis, interpretation of results, and scientific conclusions were developed and verified by the authors. The authors take full responsibility for the accuracy and integrity of the manuscript.

Data Availability Statement

Data sharing is not applicable to this article as no new datasets were generated or analysed during the current study.

Ethics Statement

This study does not involve human participants or animals. The research consists of numerical modelling and finite element simulations, and therefore ethical approval was not required.

References

Alnuaimi, H., Amjad, U., Alnuaimi, Y., & Kundu, T. (2025). Combining Ultrasonic Pulse Velocity and Nonlinear Ultrasonic Techniques to Assess Concrete Strength. *ASME J Nondestructive Evaluation 8(3)*.

Baldwin, K., Berndt, T., & Ehrlich, M. (1999). Narrowband laser generation/air coupled detection: ultrasonic system for on-line process control of composites. *Ultrasonics 37(5)*, pp 329-334.

Dixon, S., Burrows, S., Dutton, B., & Fan, Y. (2010). Detection of cracks in metal sheets using pulsed laser generated ultrasound and EMAT detection. *Ultrasonics 51*, pp 7-16.

Huang, J., Krishnaswamy, S., & Achenbach, D. (1992). Laser generation of narrow-band surface waves. *J. Acoust. Soc. Am. 92*, pp 2527-2531.

Liu, P., & Sohn, H. (2017). Development of nonlinear spectral correlation between ultrasonic modulation components. *NDT & E Int.91*, pp 120-128.

Liu, P., Jang, J., & Sohn, H. (2018). Fatigue crack detection using dual laser induced nonlinear ultrasonic modulation. *Opt. Lasers Eng.*

Liu, P., Nazirah, A., & Sohn, H. (2016). Numerical simulation of damage detection using laser-generated ultrasound. *Ultrasonics, 69*, pp 248-258.

Liu, P., Sohn, H., & Park, B. (2015). Baseline-free damage visualization using noncontact laser nonlinear ultrasonics and state space geometrical changes. *Smart Mater. Struct. 24*, pp 065036.

Liu, P., Sohn, H., Kundu, T., & Yang, S. (2014). Noncontact detection of fatigue cracks by laser nonlinear wave modulation spectroscopy (LNWMS). *NDT&E Int. 66,*, pp 106-116.

Mezil, S., Chigarev, N., Tournat, V., & Gusev, V. (2016). Evaluation of crack parameters by a nonlinear frequency-mixing laser ultrasonics method. *Ultrasonics, 69*, pp 225 235.

Murray, T., Deaton Jr, J., & Wagner, J. (1996). Experimental evaluation of enhanced generation of ultrasonic waves using an array of laser sources. *Ultrasonics 34(1)*, pp 69-77.

Park, B., An, Y., & Sohn, H. (2014). Visualization of hidden delamination and debonding in composites through noncontact laser ultrasonic scanning. *Composite Science Technology 100*, pp 10-18.

Ruzzene, M. (2007). Frequency-wavenumber domain filtering for improved damage visualization. *Smart*

Mater. Struct., 16 (6), pp 2116-2129.

Scruby, C., & Drain, L. (1990). *Laser Ultrasonics: Techniques and Applications.* London: Taylor & Francis.

Sohn, H., Dutta, D., Yang, J., Desimo, M., Olson, S., & Swenson, E. (2011). Automated detection of delamination and disbond from wavefield images obtained using a scanning laser vibrometer. *Smart Materials and Structures 20(4)*, pp 045017.

Wagner, J., Mckie, A., Spicer, J., & Deaton Jr, J. (1990). Modulated laser array sources for generation of narrowband and directed ultrasound. *J. Nondestruct. Eval. 9*, pp 263-370.

Yashiro, S., Takatsubo, J., Miyauchi, H., & Toyama, N. (2008). A novel technique for visualizing ultrasound waves in general solid media by pulsed laser scan. *NDT & E Int. 41*, pp 137-144.

Zaitsev, V., Matveev, L., & Matveyev, A. (2009). On the ultimate sensitivity of nonlinear-modulation method of crack detection. *NDT & E Int. 42*, pp 622-629.

Zhu, J., Zeng, S., Malone, C., Tu, J., & Sun, H. (2025). Thermal modulation of nonlinear ultrasonic waves for nondestructive evaluation of elastic materials. *Nondestructive Testing and Evaluation*.